Cooperative catalytic nanokinetics

Murzin, Dmitry Yu

Published in:
Chemical Engineering Science

DOI:
10.1016/j.ces.2022.117684

Published: 20/07/2022

Document Version
Final published version

Document License
CC BY

Chemical Engineering Science 256 (2022) 117684

Contents lists available at ScienceDirect

Chemical Engineering Science

journal homepage: www.elsevier.com/locate/ces

Cooperative catalytic nanokinetics

Dmitry Yu. Murzin

Åbo Akademi University, Henriksgatan 2, 20500 Åbo/Turku, Finland

HIGHLIGHTS

- Theoretical framework for cooperative kinetics on nanoclusters with several adsorbed molecules.
- Development of kinetic equations for common reaction mechanisms.
- Analysis of selectivity in consecutive and parallel reactions.
- Comparison of theory with experimental data on chemoselective hydrogenation.

ARTICLE INFO

Article history:
Received 27 February 2022
Received in revised form 2 April 2022
Accepted 16 April 2022
Available online 2 May 2022

Keywords:
Kinetics
Nanoclusters
Eley-Rideal
Langmuir-Hinshelwood
Selectivity

ABSTRACT

Cooperative kinetics of heterogeneous catalytic reactions on nanoclusters or in a nanoconfined space is considered for the Eley-Rideal and Langmuir-Hinshelwood types of mechanisms as well as for a reaction mechanism with two kinetically significant steps, by assuming few (minimum two) molecules of different type per a single metal cluster/catalytic ensemble. The treatment accounted for the lateral interactions between adsorbed species by introducing kinetic and adsorption constants dependence on the presence of adsorbed species of the same or another type. Kinetic behavior for the Eley-Rideal type of mechanism with the product adsorption was different from the classical mean –field approximation, resulting in S-shape behavior and cooperativity, while the Langmuir-Hinshelwood mechanism essentially gives the same behavior for the case of two adsorbed species of different type on a two-site ensemble. Differences in the kinetic behavior for the bimolecular mechanism compared to the conventional treatment could be seen for larger ensembles, when at least three species are adsorbed per cluster or located in a nanoconfined space.

For parallel reactions of the Eley-Rideal type, it was demonstrated that the cooperative behavior of two adsorbed molecules of a reactant per cluster results in selectivity dependence on conversion for reactions of the same order contrary to the mean field approach. In the case of consecutive reactions with such cooperative behavior, selectivity towards the intermediate product depends on the initial substrate concentration in contrast to the mean field approximation.

1. Introduction

Kinetics of heterogeneous catalytic reactions has been extensively studied along the years (Murzin and Salmi, 2016; Salmi et al., 2010; Fogler, 1998; Marin et al., 2019; Kapteijn et al., 2008; Levenspiel, 1999). The conventional approaches heavily dominating the field originate from the treatment of Langmuir, who working with metal films used an approach of ideal surfaces and applied the mass action law in a fashion similar to homogeneous reactions (Helfferich et al., 2001; Temkin, 2012). More specifically the concept of surface concentration or surface coverage assuming fast diffusion across the surface is utilized. Numerous developments were related to introduction of the concepts of lateral interactions, different reactivity of active centra with different coordination, understanding the role of substrates segregation of the solid surfaces, spatio-temporal patterns, incorporation of the polyatomic nature of reactants or the size of nanoparticles directly into the rate equations to name a few (Temkin, 1979; Rotermund et al., 1990; Bär et al., 1994; Murzin, 2010; Siffert et al., 1999).

While historically the concepts of heterogeneous catalytic kinetics have their roots in catalysis over extended surfaces (metal films or bulk catalysts, like the ones used for ammonia or methanol synthesis), nanocatalysts started to be applied already in 1910 s (Fokin, 1913; Sabatier, 2022) even if there were no readily available physico-chemical tools to elucidate the size of nanoclusters. One example is catalysis by gold (Augustine, 2016) prepared by

E-mail address: dmurzin@abo.fi

https://doi.org/10.1016/j.ces.2022.117684
0009-2509/

deposition–precipitation with urea and utilized for synthesis of formaldehyde from methanol.

From the practical viewpoint an explosion in the interest to nanocatalysts (Bell, 2003; Schlögl and Abd Hamid, 2004; Narayanan and El-Sayed, 2008; Henry, 2000; Santen, 2009; Ligthart et al., 2011; Somorjai et al., 2009; Burda et al., 2005; Astruc, 2020) was related to an increase of the metal dispersion improving catalytic activity and diminishing preparation costs and on the other hand improved accessibility to advanced characterization tools, such high resolution TEM. High metal dispersion resulting in the nanoparticles of the range of 1–2 nm, implies that only a limited number of large organic molecules can be accommodated on a single cluster, as the size of organic molecules used with industrial heterogeneous catalysts is often ca. 0.5–1 nm (Murzin, 2020).

The ultimate case of a high metal dispersion are single-atom catalysts with 100% surface utilization (Liu and Corma, 2021; Samantaray et al., 2020; Kaiser et al., 2020; Zhang et al., 2021). It is apparently clear that the concept of surface coverage loses its physical meaning as a particular catalytic site is either empty or is occupied taking part in a catalytic cycle. For such cases stochastic kinetic models based on the probability approach have been developed (Ye et al., 1985; Chen et al., 2014; Xu et al., 2008) for the Eley-Rideal kinetics borrowing the concepts (Lu et al., 1877; Kou et al., 2005) from a similar treatment for single enzymes with the so-called Michaelis-Menten kinetics (Leskovac, 2003).

An isotherm for the intermediate case, i.e. when a finite number of molecules per a single metal cluster can be adsorbed, was considered in (Murzin, 2007) and further extended (Murzin, 2010) for a two-step sequence. A general equation with polynomial terms in the nominator and the denominator was derived assuming that all kinetic and adsorption constants depend on the spatial arrangements of reacting molecules. The general form of kinetic equations allows not only saturation, typical for the Eley-Rideal kinetics, but also positive cooperativity, i.e. S shape behavior of the reaction rate r as a function of the substrate A concentration:

$$r = \frac{a_1 C_A + a_2 C_A^2 + \ldots + a_n C_A^n}{1 + b_1 C_A + b_2 C_A^2 + \ldots + b_n C_A^n} = \frac{\sum_1^n a_n C_A^n}{1 + \sum_1^n b_n C_A^n} \quad (1)$$

In Eq. (1) n is the number of adsorbed molecules per cluster, a_i stands for terms containing kinetic and adsorption constants, while b_i is related to adsorption terms. The form of equation (1) with $n + 1$ terms in the denominator is somewhat similar to the polynomial kinetics approach of Lazman and Yablonsky (Lazman and Yablonsky, 2008; Yablonsky and Lazman, 1997).

The theoretical treatment in (Murzin, 2010) was substantially simplified and mainly limited to the case of an irreversible reaction of the type A ⇒ B neglecting adsorption of the product. For a two-step sequence with a quasi-equilibrium adsorption of the reactant on the nanoclusters in the first step and subsequent transformations to a product in the second step the rate equation (1) can be simplified. For a physically reasonable case, when two molecules can be adsorbed on a cluster and when adsorption on an empty surface (K_e) and occupied surfaces (K_o) is different, the reaction rate is given by:

$$r = \frac{2k_e K_e C_A + k_0 K_o K_e C_A^2}{1 + 2K_e C_A + K_0 K_e C_A^2} \quad (2)$$

where k_e corresponds to the reaction of A when there is no neighboring molecule of A present, while k_o reflects the case when two adsorbed molecules of A are present on the surface and one of them is reacting. Numerical analysis of Eq. (2) (Murzin, 2010) demonstrated that it can lead to a maximum in the reaction rate if the ratio of these constants k_e/k_o is sufficiently high. Such maximum was discussed in (Murzin, 2010) in the context of catalytic hydrodechlorination of polychlorinated aromatics (Keane and Murzin, 2001; Keane and Murzin, 2002).

On the contrary when $k_e < k_o$, an S shape behavior, similar to cooperative enzymes (Cui and Karplus, 2008), can be also observed for heterogeneous catalysis (Murzin, 2010). Interesting cooperative behavior within and between single nanocatalysts was recently experimentally observed (Zou et al., 2018; Punia et al., 2022). On a single nanoparticle (Zou et al., 2018) such cooperativity depends on the chemical case as well as on the distance between adsorbed molecules.

While the discussion above was related to catalytic kinetics on nanoparticles, the same approach has a broader applicability and can be also utilized for other reactions in a nanoconfined space, where for example two reacting species are adsorbed on the same type of sites within a pore of a nanometer size (i.e. zeolites, nanotubes or MOFs). Nanoconfinement is mainly discussed in terms of the unique local environment (Dong et al., 2019; Dong et al., 2020) while the kinetic aspects *per se* are typically not considered. At the same time, similarly to a case of a nanoparticle of ca. 1 nm in size, just few (2 or 3) reasonably large organic molecules can be present within a nanopore.

Very recently (Razdan and Bhan, 2021; Razdan and Bhan, 2021) a simple catalytic reaction of a type 2A->A_2 was considered on site ensembles, demonstrating that even for a simple case of a site ensemble with two sites, the resulting kinetic description is different from the classical Langmuir-Hinshelwood approach.

In the current work, which is an extension of the initial theoretical treatment, presented in (Murzin, 2010), adsorption and kinetics of catalytic reactions are considered for the cases when several substrates can adsorb on the surface of an ensemble with few available sites, addressing in addition to the reaction kinetics, also the selectivity aspects. The explicit rate expressions for the Eley-Rideal as well as the Langmuir-Hinshelwood mechanisms with or without the product adsorption are considered, highlighting the differences between the mean field approximation and the current treatment.

2. Eley- Rideal mechanism

It is instructive to start first with the Eley-Rideal mechanism similar to the model presented in (Murzin, 2007; Murzin, 2010). The Eley-Rideal mechanism corresponds to a reaction between two reactants when one of them is chemisorbed, while the other one reacts from the fluid phase without chemisorption. Different options within the framework of this mechanism exist for adsorption behavior of the product. The main difference of the current treatment compared to the previous considerations (Murzin, 2010) of only one abundant surface species and an irreversible reaction, is that hereby besides adsorption of the reactant A and a subsequent reaction with B, also adsorption of the product C on a surface site * is considered for an overall reversible reaction. The mechanism thus takes the form:

$$\begin{aligned} &1.\ * + A = *A \\ &2.\ *A + B <-> *C \\ &\underline{3.\ *C = * + C} \\ &A + B <-> C \end{aligned} \quad (3)$$

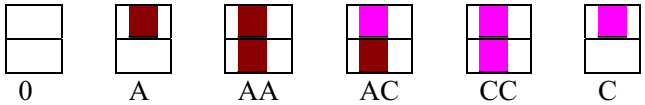

Fig. 1. Clusters with up to two adsorbed species of different types for the mechanism in Eq. (3).

In Eq. (3) steps 1 and 3 are at quasi-equilibria, which is specified by the sign =.

For a simple case of a nanoconfined space with maximum two adsorbed species per cluster several arrangements are possible on the surface as illustrated in Fig. 1.

An expression for adsorption equilibrium of the reactant A on a bare cluster is given as:

$$K_{0A} = \frac{f_{0A}}{f_{00}C_A} f_{0A} = K_{0A} f_{00} C_A \tag{4}$$

where K_{0A} is the equilibrium constant for such adsorption, f_{00} and f_{0A} are, respectively, the concentration of bare clusters, and those clusters, which can adsorb only one reactant A per cluster. The cluster containing one adsorbed molecule can accommodate another molecule of the same reactant with an equilibrium constant different from K_{0A} in a general case, if there are some lateral interactions between these two molecules:

$$K_{AA} = \frac{f_{AA}}{f_{0A}C_A} f_{AA} = K_{AA} f_{0A} C_A = K_{0A} K_{AA} f_{00} {C_A}^2 \tag{5}$$

In a similar fashion for the equilibrium constant for adsorption of the product C one gets:

$$f_{0C} = K_{0C} f_{00} C_C f_{CC} = K_{0C} K_{CC} f_{00} C_C^2 \tag{6}$$

The last remaining option is the situation of simultaneous adsorption of the reactant and the product in that sequence:

$$K_{AC} = \frac{f_{AC}}{f_{0A}C_C} = \frac{f_{AC}}{K_{0A} f_{00} C_A C_C} f_{AC} = K_{AC} K_{0A} f_{00} C_A C_C \tag{7}$$

An alternative sequence of the reactant adsorption on a cluster bearing the product gives:

$$K_{CA} = \frac{f_{CA}}{f_{0C}C_A} = \frac{f_{AC}}{K_{0C} f_{00} C_A C_C} f_{CA} = K_{CA} K_{0C} f_{00} C_A C_C \tag{8}$$

This case implies presence of lateral interactions in the spirit of Fowler-Guggenheim or Frumkin adsorption isotherms, as adsorption depends on the composition of the adsorbed layer. The treatment above distinguishes clusters with both the reactant and the product adsorbed depending on the sequence of adsorption steps. In a special case of non– distinguishable clusters$K_{CA}K_{0C} = K_{AC}K_{0A}$.

The balance equation relating the concentration of clusters with the total amount of clusters f_{total} is written as:

$$f_{00} + f_{0A} + f_{AA} + f_{0C} + f_{CC} + f_{AC} + f_{CA} = f_{total} \tag{9}$$

Giving thus:

$$f_{00} = \frac{f_{total}}{1 + K_{0A}C_A + K_{0A}K_{AA}C_A^2 + K_{0C}C_C + K_{0C}K_{CC}C_C^2 + (K_{AC}K_{0A} + K_{CA}K_{0C})C_A C_C} \tag{10}$$

In the denominator in Eq. (10) the term comprising concentrations of the reactant and the product $(K_{AC}K_{0A} + K_{CA}K_{0C})C_A C_C$ will have a degeneracy factor equal to two, when lateral interactions are absent (e.g. $(K_{AC}K_{0A} + K_{CA}K_{0C}) = 2K'_A K'_C$).

The forward reaction proceeds through transformations of *A*, *AA* and *AC* present on the corresponding clusters leading to the rate expression with fractional cluster concentrations (equivalent to coverage in a classical treatment):

$$r_+ = (k_A f_{0A} + 2k_{AA} f_{AA} + k_{AC} f_{AC} + k_{CA} f_{CA}) C_B / f_{total} \tag{11}$$

where the term $2k_{AA}f_{AA}$ is present as two products can be formed starting from a cluster with two adsorbed molecules of the reactant.

Subsequent manipulations with Eq. (11) result in:

$$r_+ = \frac{(k_A K_{0A} C_A + 2k_{AA} K_{0A} K_{AA} C_A^2 + (k_{AC} K_{AC} K_{0A} + k_{CA} K_{CA} K_{0C}) C_A C_C) C_B}{1 + K_{0A}C_A + K_{0A}K_{AA}C_A^2 + (K_{AC}K_{0A} + K_{CA}K_{0C})C_A C_C + K_{0C}C_C + K_{0C}K_{CC}C_C^2} \tag{12}$$

Considering an expression for the overall rate of a single route reaction:

$$r = r_+ - r_- = r_+ \left(1 - \frac{r_-}{r_+}\right) \tag{13}$$

the ratio between the rates in the reverse and forward direction can be easily obtained from the general treatment of Horiuti and Boreskov (Marin et al., 2019; Boreskov et al., 1945; Horiuti and Enomoto, 1953). In a special case of a reversible reaction without a rate-limiting step and the stoichiometric number of all steps equal to unity, the general expression (Temkin, 1963) is simplified to:

$$\frac{r_-}{r_+} = \frac{1}{K} \frac{C_C}{C_A C_B} \tag{14}$$

The reaction in Eq. (3) in fact comprises four routes reflected by 4 terms in the numerator of Eq. (12) with the same overall chemical equation and thus the same equilibrium constant for each route. Subsequently the overall reaction for the scheme in Eq. (3) with two available sites on a cluster or in a nanoconfined space can be expressed by the following rate equation:

$$r = \frac{(k_A K_{0A} C_A + 2k_{AA} K_{0A} K_{AA} C_A^2 + (k_{AC} K_{AC} K_{0A} + k_{CA} K_{CA} K_{0C}) C_A C_C) C_B}{1 + K_{0A}C_A + K_{0A}K_{AA}C_A^2 + (K_{AC}K_{0A} + K_{CA}K_{0C})C_A C_C + K_{0C}C_C + K_{0C}K_{CC}C_C^2} \times \left(1 - \frac{1}{K}\frac{C_C}{C_A C_B}\right) \tag{15}$$

This equation in a very general form contains different kinetic and adsorption constants which depend on the spatial arrangements of reacting molecules, namely on the presence of adsorbed species of another type. If this is not the case, Eq. (15) can be essentially simplified:

$$r = \frac{k_A (K_A C_A + 2K_A^2 C_A^2 + 2K_A K_C C_A C_C) C_B}{1 + K_A C_A + K_A^2 C_A^2 + 2K_A K_C C_A C_C + K_C C_C + K_C^2 C_C^2} \left(1 - \frac{1}{K}\frac{C_C}{C_A C_B}\right) \tag{16}$$

It is apparently clear from Eq. (15) that depending on the values of the rate and adsorption constants, different behavior can be expected for the forward rate including the second order in the reactant *A* or even a maximum in the rate upon an increase in the reactant *A* concentration. The latter case is possible if the transformation rate of A to C is diminished due to the lateral interactions between two molecules of *A* (i.e. $k_A > k_{AA}$). A similar situation with the corresponding numerical simulations was discussed already in (Murzin, 2010) where it was mentioned that presence of several adsorbed reactants on a cluster can lead to the rate maxima even for the forward reaction in contrast to the conventional Eley-Rideal mechanism. In the latter case the reaction order in the forward direction for the reactant coming from the fluid phase is equal to unity, similar to Eq. (16), however, the reaction order for the chemisorbed reactant (i.e. A) changes between one and zero upon elevation of this reactant concentration.

Occurrence of several terms containing the product *C* concentration in the denominator of Eq. (15) and (16) might lead to the rate retardation, as expected. Less obvious is a potential positive influence of the product *C* on the reaction rate as its concentration appears also in the numerator of Eq. (15). This implies a possible S-shape behavior of the rate vs the substrate concentration when the rate is low at low substrate concentration levels while somewhat higher concentrations result in a much steeper dependence with

eventual flattening out towards the maximal velocity or even giving a maximum in the rate.

It was previously demonstrated (Murzin, 2010) that Eq. (15) can lead to a rate maximum as a function of the reactant concentration when there some sort of positive cooperativity with significant changes in the rate constant due to lateral interactions (e.g. for the current case $k_A << k_{AA}$). In fact, such maximum can result even for the case when the transformation rate does not depend on the presence of another reactant molecule on the surface.

Let us consider Eq. (16) at a low surface coverage, which implies that$1 > K_AC_A + K_A^2C_A^2 + 2K_AK_CC_AC_C + K_CC_C + K_C^2C_C^2$, resulting therefore in an expression for the rate in the forward direction:

$$r_+ = k_A(K_AC_A + 2K_A^2C_A^2 + 2K_AK_CC_AC_C)C_B = \\ = k_AK_AC_BC_A(1 + 2K_CC_A^0) + 2k_AK_AC_BC_A^2(K_A - K_C) \quad (17)$$

For the derivation of Eq. (17) it was considered that$C_C = C_A^0 - C_A$, where C_A^0 is the initial concentration of the reactant *A*. Taking the first derivative of the rate in Eq. (17) and letting in be equal to zero, a concentration of *A* at which the rate passes the maximum can be easily obtained:

$$C_{A\_at\_\max} = \frac{1 + 2K_CC_A^0}{4(K_C - K_A)} \quad (18)$$

The value of this concentration is positive and thus the rate indeed can pass through a maximum when the product is adsorbed stronger than the reactant, even in the absence of positive cooperativity for the rate constants.

3. Two step sequence

A somewhat similar to the Eley-Rideal mechanism is the two step sequence often used to describe experimental data in heterogeneous catalysis (Temkin, 1984; Boudart and Tamaru, 1991).

$$1. * + A \leftrightarrow I * + C \\ 2. I * + C \leftrightarrow * + D \\ A + B <-> C + D \quad (19)$$

where *A, B, C* and *D* are reactants, and *I* is an adsorbed intermediate. Both steps in the mechanism (19) are reversible. For this case, just three options of adsorbed species arrangement on the catalyst surface are possible (Fig. 2).

Eq. (19) can be rewritten in a slightly different way:

	$N^{(I)}$	$N^{(I')}$
1. *+A↔I*+C	1	0
2. I* +B↔* +D	1	0
1'.I* +A↔II* +C	0	1
2'. II*+B↔I*+D	0	1
$N^{(I)}$, $N^{(I')}$: A+B ↔ C+D		

(20)

where the numbers (0 or 1) correspond to the stoichiometric numbers (i.e. Horiuti numbers) of a particular step in the corresponding reaction route (Temkin, 1979). There are two reaction routes in Eq. (20) giving the same chemical equation. The concentration of the f_0, f_1, and f_2 can be calculated based on the steady state approximation for both reaction routes:

$$r_{+1} - r_{-1} = r_{+2} - r_{-2} \quad (21)$$

$$r'_{+1} - r'_{-1} = r'_{+2} - r'_{-2} \quad (22)$$

Or

$$k_{+1}C_Af_0 - k_{-1}C_Cf_1 = k_{+2}C_Bf_1 - k_{-2}C_Df_0 \quad (23)$$

$$k'_{+1}C_Af_1 - k'_{-1}C_Cf_2 = k'_{+2}C_Bf_2 - k'_{-2}C_Df_1 \quad (24)$$

Giving subsequently:

$$f_1 = U_1f_0f_2 = U_1U_2f_0 \quad (25)$$

where U_1 and U_2 are expressed through the frequencies of steps (e.g.$\omega_{+1}^0 = k_{+1}C_A$, etc.):

$$U_1 = \frac{k_{+1}C_A + k_{-2}C_D}{k_{+2}C_B + k_{-1}C_C} = \frac{\omega_{+1}^0 + \omega_{-2}^0}{\omega_{+2}^0 + \omega_{-1}^0} \quad (26)$$

$$U_2 = \frac{k'_{+1}C_A + k'_{-2}C_D}{k'_{+2}C_B + k'_{-1}C_C} = \frac{\omega'_{+1} + \omega'_{-2}}{\omega'_{+2} + \omega'_{-1}} \quad (27)$$

Note that there were typing errors in a similar expression for *U* developed in (Murzin, 2010) for the case when the rate constants are the same on bare and occupied clusters and the sign "-" appeared instead of sign "+" in both the numerator and denominator. Such error did not influence the conclusions and the overall treatment as the general expression contained the term *U*, while the numerical data fitting was done for the irreversible case.

The concentration of the clusters free from adsorbed species can be obtained from the mass balance of sites:

$$f_0 + f_1 + f_2 = f_{total} \quad (28)$$

resulting in the expression for the bare clusters concentration:

$$f_0 = \frac{f_{total}}{1 + U_1 + U_1U_2} \quad (29)$$

The overall reaction rate along two routes is the sum of the rates of these routes (Temkin, 1979):

$$r = r^{(I)} + r^{(I')} = r_{+1} - r_{-1} + r'_{+1} - r'_{-1} = \omega_{+1}^0f_o - \omega_{-1}^0f_1 + \omega_{+1}^1f_1 - \omega_{-1}^1f_2 \quad (30)$$

Combining Eq. (30) with (29) one gets:

$$r = \frac{(\omega_{+1}^0 + \omega_{+1}^1U_1 - \omega_{-1}^0U_1 - \omega_{-1}^1U_1U_2)f_{total}}{1 + U_1 + U_1U_2} \quad (31)$$

which, for a simple case of two irreversible steps using the expressions (26) and (27), is transformed into an equation for the forward reaction:

$$r_+ = \frac{(\omega_{+1}^0 + \omega'_{+1}\frac{\omega_{+1}^0}{\omega_{+2}^0})f_{total}}{1 + \frac{\omega_{+1}^0}{\omega_{+2}^0} + \frac{\omega_{+1}^0}{\omega_{+2}^0}\frac{\omega'_{+1}}{\omega'_{+2}}} \quad (32)$$

leading finally to the rate of the two-step sequence with both irreversible steps:

$$r_+ = \frac{(k_{+1}k_{+2}C_AC_B^2 + k_{+1}k'_{+1}C_BC_A^2)f_{total}}{k_{+1}C_AC_B + k_{+2}C_B^2 + k_{+1}\frac{k'_{+1}}{k'_{+2}}C_A^2} \\ = \frac{(k_{+1}k_{+2}C_AC_B + k_{+1}k'_{+1}C_A^2)f_{total}}{k_{+1}C_A + k_{+2}C_B + k_{+1}\frac{k'_{+1}}{k'_{+2}}\frac{C_A^2}{C_B}} \quad (33)$$

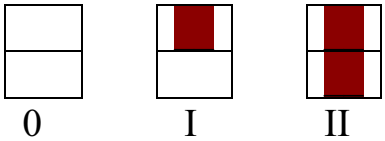

Fig. 2. Clusters with up to two adsorbed species of different type for the mechanism in Eq. (19).

This expression can be easily reduced to the one well known for the two-step sequence with both irreversible steps by simply setting $k'_{+1} = 0$:

$$r_+ = \frac{k_{+1}k_{+2}C_AC_Bf_{total}}{k_{+1}C_A + k_{+2}C_B} \tag{34}$$

For a general case of both reversible steps Eq. (31) leads to a slightly more complicated expression:

$$r = \frac{(\omega^0_{+1}\omega^0_{+2} - \omega^0_{-1}\omega^0_{-2} + (\omega'_{+1}\omega'_{+2} - \omega'_{-1}\omega'_{-2})\frac{\omega^0_{+1}+\omega^0_{-2}}{\omega'_{+2}+\omega'_{-1}})f_{total}}{\omega^0_{+1} + \omega^0_{+2} + \omega^0_{-1} + \omega^0_{-2} + (\omega^0_{+1} + \omega^0_{-2})\frac{\omega'_{+1}+\omega'_{-2}}{\omega'_{+2}+\omega'_{-1}}} \tag{35}$$

which is reduced to Eq. (32) by setting the values of step frequencies equal to zero for all steps in the backward direction.

The classical rate expression for the two- step mechanism (Temkin, 1979) can be also obtained from Eq. (35) by setting the values of frequencies for the second route equal to zero:

$$r = \frac{(\omega^0_{+1}\omega^0_{+2} - \omega^0_{-1}\omega^0_{-2})f_{total}}{\omega^0_{+1} + \omega^0_{+2} + \omega^0_{-1} + \omega^0_{-2}} \tag{36}$$

The reaction rate of the overall reaction in Eq. (35) can be also expressed through the rate in the forward direction:

$$r = r_+(1 - \frac{1}{K}\frac{C_CC_D}{C_AC_B}) \tag{37}$$

where

$$r_+ = \frac{(\omega^0_{+1}\omega^0_{+2} + \omega'_{+1}\omega'_{+2}\frac{\omega^0_{+1}+\omega^0_{+2}}{\omega'_{+2}+\omega'_{-1}})f_{total}}{\omega^0_{+1} + \omega^0_{+2} + \omega^0_{-1} + \omega^0_{-2} + (\omega^0_{+1} + \omega^0_{-2})\frac{\omega'_{+1}+\omega'lv}{\omega'_{+2}+\omega'_{-1}}} \tag{38}$$

Let us analyse the partial reaction order for a case of two irreversible steps expressed through Eq. (33).

The apparent reaction order is defined as:

$$n_{A,app} = \frac{\partial \ln(r/f_{total})}{\partial \ln C_A} = \frac{\partial \ln(k_{+1}k_{+2}C_AC_B + k_{+1}k'_{+1}C_A^2)}{\partial \ln C_A} - \frac{\partial \ln(k_{+1}C_A + k_{+2}C_B + k_{+1}\frac{k'_{+1}C_A^2}{k'_{+2}C_B})}{\partial \ln C_A} =$$
$$= \frac{\partial \ln C_A}{\partial \ln C_A} + \frac{\partial \ln(k_{+1}k_{+2}C_B + k_{+1}k'_{+1}C_A)}{\partial \ln C_A} - \frac{\partial \ln(k_{+1}C_A + k_{+2}C_B + k_{+1}\frac{k'_{+1}C_A^2}{k'_{+2}C_B})}{\partial \ln C_A} \tag{39}$$

which after some transformations gives:

$$n_{A,app} = 1 + C_A\frac{\frac{\partial(k_{+1}k_{+2}C_B + k_{+1}k'_{+1}C_A)}{\partial C_A}}{k_{+1}k_{+2}C_B + k_{+1}k'_{+1}C_A} - C_A\frac{\frac{\partial(k_{+1}C_A + k_{+2}C_B + k_{+1}\frac{k'_{+1}C_A^2}{k'_{+2}C_B})}{\partial C_A}}{k_{+1}C_A + k_{+2}C_B + k_{+1}C_A\frac{k'_{+1}C_A}{k'_{+2}C_B}} =$$
$$= 1 + \frac{k'_{+1}C_A}{k_{+2}C_B + k'_{+1}C_A} - \frac{k_{+1}C_A + 2k_{+1}\frac{k'_{+1}C_A^2}{k'_{+2}C_B}}{k_{+1}C_A + k_{+2}C_B + k_{+1}C_A\frac{k'_{+1}C_A}{k'_{+2}C_B}} \tag{40}$$

When the value of $k'_{+1} \approx 0$ Eq. (40) is reduced to the one corresponding to the classical two-step sequence (Marin et al., 2019) (i.e. just the route N(I) in Eq. (20)):

$$n_{A,app} = 1 - \frac{k_{+1}C_A}{k_{+1}C_A + k_{+2}C_B} = \frac{k_{+2}C_B}{k_{+1}C_A + k_{+2}C_B} = 1 - \theta_I \tag{41}$$

Under the excess of the reactant B when $k_{+2}C_B$ exceeds other terms on the denominators of Eq. (40) the apparent reaction order towards component A is:

$$n_{A,app} = 1 + \frac{k'_{+1}C_A(1 - \frac{2k_{+1}}{k'_{+2}}\frac{C_A}{C_B}) - k_{+1}C_A}{k_{+2}C_B} \tag{42}$$

For high concentrations of the reactant A, Eq. (40) after some simplifications will result in the zero order towards this reactant.

$$n_{A,app} \approx 1 + \frac{k'_{+1}C_A}{k'_{+1}C_A} - \frac{k_{+1}C_A + 2k_{+1}\frac{k'_{+1}}{k'_{+2}}\frac{C_A^2}{C_B}}{k_{+1}C_A + k_{+1}\frac{k'_{+1}}{k'_{+2}}\frac{C_A^2}{C_B}}$$
$$\approx 2 - \frac{k_{+1}C_A + 2k_{+1}\frac{k'_{+1}}{k'_{+2}}\frac{C_A^2}{C_B}}{k_{+1}C_A + k_{+1}\frac{k'_{+1}}{k'_{+2}}\frac{C_A^2}{C_B}} \approx 0 \tag{43}$$

as could be anticipated.

A similar analysis for the substrate B as for the reactant A:

$$n_{B,app} = \frac{\partial \ln(r/f_{total})}{\partial \ln C_B} = \frac{\partial \ln(k_{+1}k_{+2}C_AC_B^2 + k_{+1}k'_{+1}C_BC_A^2)}{\partial \ln C_B} - \frac{\partial \ln(k_{+1}C_AC_B + k_{+2}C_B^2 + k_{+1}\frac{k'_{+1}}{k'_{+2}}C_A^2)}{\partial \ln C_B} =$$
$$= \frac{\partial \ln C_B}{\partial \ln C_B} + \frac{\partial \ln(k_{+1}k_{+2}C_AC_B + k_{+1}k'_{+1}C_A^2)}{\partial \ln C_B} - \frac{\partial \ln(k_{+1}C_AC_B + k_{+2}C_B^2 + k_{+1}\frac{k'_{+1}}{k'_{+2}}C_A^2)}{\partial \ln C_B} \tag{44}$$

gives the apparent reaction order for this component:

$$n_{B,app} = 1 + C_B\frac{\frac{\partial(k_{+1}k_{+2}C_AC_B + k_{+1}k'_{+1}C_A^2)}{\partial C_B}}{k_{+1}k_{+2}C_AC_B + k_{+1}k'_{+1}C_A^2} - C_B\frac{\frac{\partial(k_{+1}C_AC_B + k_{+2}C_B^2 + k_{+1}\frac{k'_{+1}}{k'_{+2}}C_A^2)}{\partial C_B}}{k_{+1}C_AC_B + k_{+2}C_B^2 + k_{+1}\frac{k'_{+1}}{k'_{+2}}C_A^2} =$$
$$= 1 + \frac{k_{+2}C_B}{k_{+2}C_B + k'_{+1}C_A} - \frac{k_{+1}C_AC_B + 2k_{+2}C_B^2}{k_{+1}C_AC_B + k_{+2}C_B^2 + k_{+1}\frac{k'_{+1}}{k'_{+2}}C_A^2} \tag{45}$$

The overall reaction order can be computed as a sum of the apparent reaction orders to the components (Marin et al., 2019). In the case of the reactions in a nanoconfined space for the two-step with both irreversible steps (Eq. (40) and (45)) it holds that the overall order is equal to unity similar to the conventional derivation for such case following the classical Langmuir approach (Marin et al., 2019):

$$\sum n_{app} = 2 + \frac{k_{+2}C_B + k'_{+1}C_A}{k_{+2}C_B + k'_{+1}C_A} - 2\frac{k_{+1}C_AC_B + k_{+2}C_B^2 + k_{+1}\frac{k'_{+1}}{k'_{+2}}C_A^2}{k_{+1}C_AC_B + k_{+2}C_B^2 + k_{+1}\frac{k'_{+1}}{k'_{+2}}C_A^2} = 1 \tag{46}$$

4. Langmuir-Hinshelwood mechanism

A somewhat simplified case of this mechanism will be considered below assuming fast desorption of the product and overall irreversibility.

$$\begin{aligned} &1. * + A = *A \\ &2. * + B = *B \\ &3. *A + *B -> 2* + C \\ &\quad A + B -> C \end{aligned} \tag{47}$$

The conventional definition of the Langmuir-Hinshelwood mechanism, which separates it from the Eley-Rideal mechanism, is the suggestion that in a reaction between two kinds of molecules on a surface, both are adsorbed on the surface of a catalyst. Note that Langmuir himself considered both mechanisms for oxidation of CO, as pointed out in (Temkin, 1979).

For a simple case of nanoconfined space with maximum two adsorbed species per cluster the possible arrangements are shown in Fig. 3, which is similar to Fig. 1, but with different notation for adsorbed species.

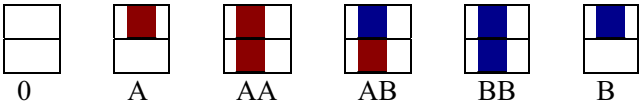

Fig. 3. Clusters with up to two adsorbed species of different type on a two-site ensemble corresponding to the mechanism in Eq. (47).

Similar to the case of the Eley-Rideal mechanism, the concentration of clusters with adsorption of either of the reactants is:

$$f_{0A} = K_{0A}f_{00}C_A f_{AA} = K_{0A}K_{AA}f_{00}C_A{}^2 \quad f_{0B} = K_{0B}f_{00}C_B f_{BB} = K_{0B}K_{BB}f_{00}C_B^2 \tag{48}$$

where for example f_{00} and f_{0A} are, respectively, the concentration of bare clusters, and those clusters, which, can adsorb only one reactant A per cluster.

In the case when co-adsorption depends on the sequence of adsorption events one gets:

$$f_{AB} = K_{AB}K_{0A}f_{00}C_A C_B f_{BA} = K_{BA}K_{0B}f_{00}C_A C_B \tag{49}$$

The balance equation for the clusters is similar to the one for the Eley-Rideal case (Eq. (10)) taking the form:

$$f_{00} = \frac{f_{total}}{1 + K_{0A}C_A + K_{0A}K_{AA}C_A^2 + K_{0B}C_B + K_{0B}K_{BB}C_B^2 + (K_{AB}K_{0A} + K_{BA}K_{0B})C_A C_B} \tag{50}$$

The reaction rate for the overall reaction is equal to the rate of the forward reaction as step 3 in mechanism (47) is irreversible:

$$r_+ = (k_{AC}f_{AC} + k_{CA}f_{CA})/f_{total} \tag{51}$$

$$r_+ = \frac{(k_{AB}K_{AB}K_{0A} + k_{BA}K_{BA}K_{0B})C_A C_B}{1 + K_{0A}C_A + K_{0A}K_{AA}C_A^2 + K_{0B}C_B + K_{0B}K_{BB}C_B^2 + (K_{AB}K_{0A} + K_{BA}K_{0B})C_A C_B} \tag{52}$$

Eq. (52) is slightly different from a classical Langmuir-Hinshelwood approach, which for an irreversible reaction gives:

$$r_+ = \frac{kK_A K_B C_A C_B}{(1 + K_A C_A + K_B C_B)^2} \tag{53}$$

Obviously at low concentrations of both reagents Eq. (52), reflecting catalytic reactions on a nanocluster or in a nanoconfined space capable of accommodating two adsorbed molecules, results in the first order kinetic as is the case if a classical Langmuir-Hinshelwood expression for a bimolecular reaction Eq. (53).

In fact, Eq. (53) is very similar to Eq. (52) different just in the meaning of the parameters for those terms, which contain concentrations of the reactants. Differences in the kinetic behavior for the mechanism in Eq. (47) compared to the classical Langmuir-Hinshelwood mechanism could be anticipated for a larger cluster, where even three species can be adsorbed per cluster (Fig. 4).

A simplified analysis of the kinetics corresponding to the mechanism (47) with the distribution of adsorbed species as illustrated in Fig. 4 can be done by neglecting lateral interactions for the adsorption and kinetic parameters, which results in the rate for the forward reaction:

$$r_+ = \frac{k(K_A K_B C_A C_B + K_A^2 K_B C_A^2 C_B + K_A K_B^2 C_A C_B^2)}{1 + K_A C_A + K_A^2 C_A^2 + K_A^3 C_A^3 + K_B C_B + K_B^2 C_B^2 + K_B^3 C_B^3 + K_A K_B C_A C_B + K_A^2 K_B C_A^2 C_B + K_A K_B^2 C_A C_B^2} = \frac{kK_A K_B C_A C_B(1 + K_A C_A + K_B C_B)}{1 + K_A C_A + K_A^2 C_A^2 + K_A^3 C_A^3 + K_B C_B + K_B^2 C_B^2 + K_B^3 C_B^3 + K_A K_B C_A C_B + K_A^2 K_B C_A^2 C_B + K_A K_B^2 C_A C_B^2} \tag{54}$$

At a low coverage of adsorbed species, Eq. (54) is reduced to an overall second order equation with the first order for each component. High affinity of one reactant (i.e. A) to the surface and its high concentration, giving$K_A C_A >> 1 + K_B C_B$, result in a negative order towards this reactant similar to the classical treatment. Negative orders to the reactants at high concentrations follow for both expressions, however, Eq. (54) exhibits higher flexibility in terms of apparent reaction orders.

It is worth to compare the Eley-Rideal reaction mechanism with the kinetic expression stemming from the Langmuir-Hinshelwood counterpart. To this end, only the forward reaction in Eq. (15) can be considered, neglecting also adsorption of the product. This leads after a straightforward procedure to the following expression:

$$r_+ = \frac{(k_A K_{0A} C_A + 2k_{AA}K_{0A}K_{AA}C_A^2)C_B}{1 + K_{0A}C_A + K_{0A}K_{AA}C_A^2} \tag{55}$$

A somewhat similar equation was derived in (Bär et al., 1994). As clearly follows from Eq. (55) high concentrations of the substrate A eventually result in the reaction order towards this compound equal to zero, while an order above unity is possible at low concentrations in the case of rate acceleration when one substrate molecule is already present on the cluster. Such behavior is distinct from the one following from the Langmuir-Hinshelwood kinetics on a two-site nanocluster as the maximum reaction order in each compound cannot exceed unity.

The treatment above considered the so-called Langmuir-Hinshelwood mechanism with competitive adsorption. Extension of this analysis can be also done for the nocompetitive adsorption with a site ensemble in a simplified case consisting of two sites for one reactant and two for the other (Fig. 5) assuming negligible adsorption of the product.

The concentration of clusters with adsorption of either of the reactants is given by Eq. (48) neglecting inter-cluster lateral interactions. From the balance equations for the clusters in such case the concentration of clusters without any adsorbed species are:

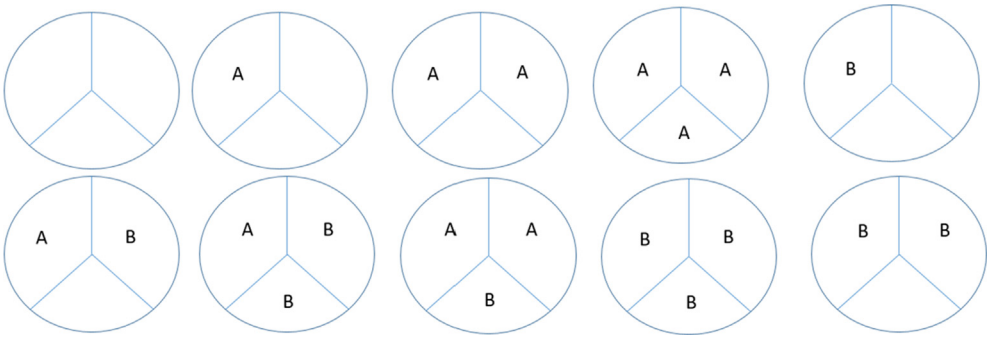

Fig. 4. Clusters with up to three adsorbed species of different type on a two- site ensemble corresponding to the mechanism in Eq. (47).

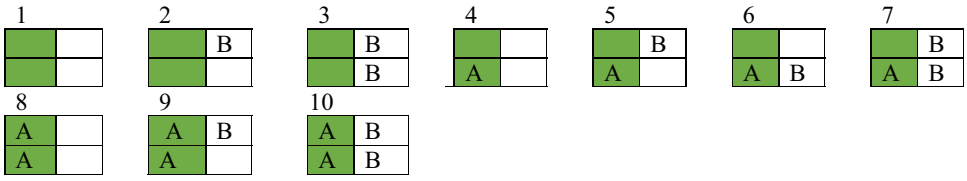

Fig. 5. Clusters with up to two adsorbed species on an ensemble with two adjacent pairs of different two sites ensembles.

$$f_{00} = \frac{f_{total}}{1 + K_{0A}C_A + K_{0A}K_{AA}C_A^2} \tag{56}$$

$$f'_{00} = \frac{f'_{total}}{1 + K_{0B}C_B + K_{0B}K_{BB}C_B^2} \tag{57}$$

Eqs. (56) and (57) imply that the reactant *A* is adsorbed on one type of the site ensemble while another site ensemble (denoted with the sign ‘) accommodates the reactant B. The reaction rate for the case of the irreversible reaction with noncompetitive adsorption of reactants is equal to:

$$r_+ = \frac{k^{adj}_{0A,0B}f_{0A}f_{0B}}{f_{total}f'_{total}} + \frac{k^{opp}_{0A,0B}f_{0A}f_{0B}}{f_{total}f'_{total}} + \frac{k_{0A,BB}f_{0A}f_{BB}}{f_{total}f'_{total}} + \frac{k_{AA,0B}f_{AA}f_{0B}}{f_{total}f'_{total}} + 2 \times \frac{k_{AA,BB}f_{AA}f_{BB}}{f_{total}f'_{total}} \tag{58}$$

considering all possible configurations of adsorbed species. Moreover, the first two terms explicitly distinguish between adjacent adsorbed species (case 6) and those with a larger distance between adsorbates (case 5 in Fig. 5). The last term in Eq. (58) accounts for two products, which can be formed in the case of arrangement 10 in Fig. 5. From Eq. (58) the rate expression for the bimolecular reaction with noncompetitive adsorption on site ensembles with two sites can be obtained:

$$r_+ = \frac{kC_AC_B + k'C_AC_B^2 + k''C_A^2C_B + k'''C_A^2C_B^2}{(1 + K_{0A}C_A + K_{0A}K_{AA}C_A^2)(1 + K_{0B}C_B + K_{0B}K_{BB}C_B^2)} \tag{59}$$

with

$$k = (k^{adj}_{0A,0B} + k^{opp}_{0A,0B})K_{0A}K_{0B}; k' = k_{0A,BB}K_{0A}K_{0B}K_{BB}; \quad k'' = k_{AA,0B}K_{0A}K_{AA}K_{0B}; k''' = 2k_{AA,BB}K_{0A}K_{AA}K_{0B}K_{BB} \tag{60}$$

Eq. (59), which in a special case can be easily reduced to a classical Langmuir-Hinshelwood kinetics with noncompetitive adsorption:

$$r_+ = \frac{kC_AC_B}{(1 + K_{0A}C_A)(1 + K_{0B}C_B)} \tag{61}$$

otherwise, has a more rich kinetic behavior compared to Eq. (61).

Applicability of the theoretical treatment discussed above is interesting to verify for a case of a catalytic reaction clearly deviating from conventional kinetics of Eley-Rideal and Langmuir-Hinshelwood mechanisms. To this end catalytic hydrodechlorination of polychlorinated aromatics namely 1,3-dichlorobenzene will be considered below based on the data reported in the literature (Keane and Murzin, 2001; Keane and Murzin, 2002) for Ni on silica with the surface average nickel diameter of 1.4 nm. Previously similar analysis was done for hydrodechlorination of 1,2-dichlorobenzene (Murzin, 2010) in the case of Eley-Rideal mechanism without, however, any comparison of rival mechanisms. As can be seen from the experimental data presented in Fig. 6 the hydrodechlorination rate dependence on dichlorobenzene partial pressure exhibits maxima at all studied temperatures. At lower partial pressures of the reactant an S-shaped behavior is visible with the reaction order exceeding unity and approaching two. The classical Eley-Rideal or Langmuir-Hinshelwood type of expressions apparently cannot describe such behavior. The rate expression capable of describing such kinetic regularities should include at least a reaction order equal to 2 in the numerator and a term with the reaction order of 3 in the denominator. The simplest equation satisfying these requirements is Eq. (54), possessing in a lumped form five parameters.

The assumption of three adsorbed species per cluster is physically reasonable considering the size of the reactant and the size of a nickel cluster.

Fig. 6a clearly demonstrates applicability of this equation to describe the experimental data even if the system is clearly overparametrized. An alternative Eley-Rideal mechanism assumes that hydrogen reacts directly from the gas phase and in case of three adsorbed species per cluster should have three terms in the numerator (first, second and third order in the substrate) and three terms of the same order in the denominator in addition to unity (Fig. 6b). As visible from Fig. 6b it is more challenging to have a description of the rate maxima, moreover the Eley-Rideal mechanism statistically is less adequate.

5. Selectivity in parallel reactions

Selectivity analysis in parallel reactions giving two products:

corresponding for example to hydrogenation of an organic compound with two functional groups, will be analyzed below for an irreversible reaction with fast desorption of both products. The kinetic equations for both reactions are similar to Eq. (56) namely:

$$r_{+1} = \frac{(k_A^{(1)}K_{0A}C_A + 2k_{AA}^{(1)}K_{0A}K_{AA}C_A^2)C_B}{1 + K_{0A}C_A + K_{0A}K_{AA}C_A^2}; \quad r_{+2} = \frac{(k_A^{(2)}K_{0A}C_A + 2k_{AA}^{(2)}K_{0A}K_{AA}C_A^2)C_B}{1 + K_{0A}C_A + K_{0A}K_{AA}C_A^2} \tag{62}$$

Strictly speaking even the values of adsorption constants for two parallel routes can be different as the modes of adsorption for reactants with several functional groups (i.e. C = C and C = O) can vary. For the purpose of the current treatment, focusing exclusively on selectivity, such distinction can be relaxed.

From the differential equations for the products concentrations vs time it naturally follows that the ratio of the products and thus selectivity depends on the concentration of the substrate (i.e. conversion):

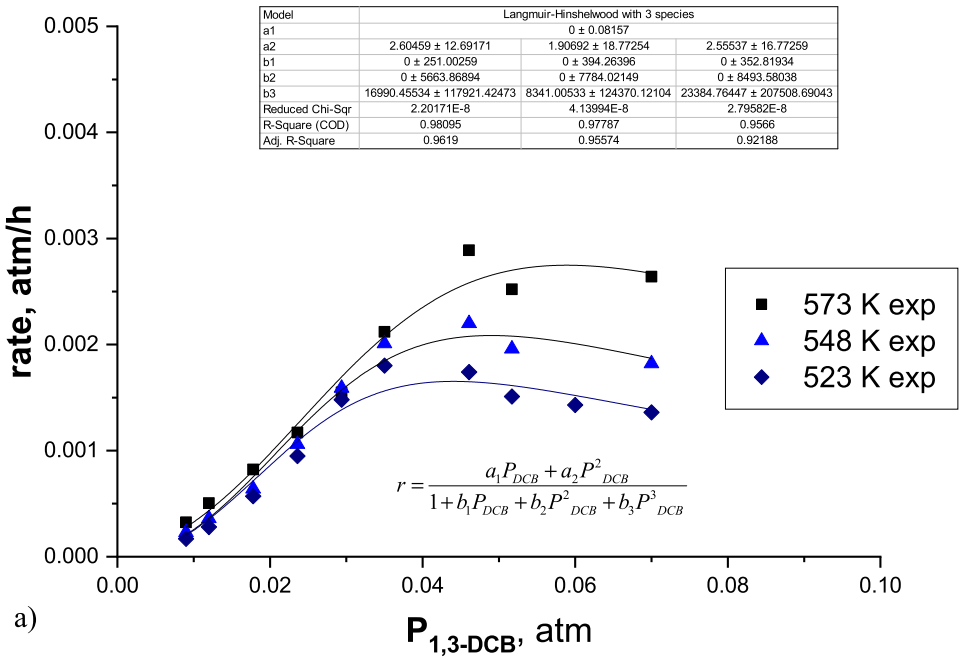

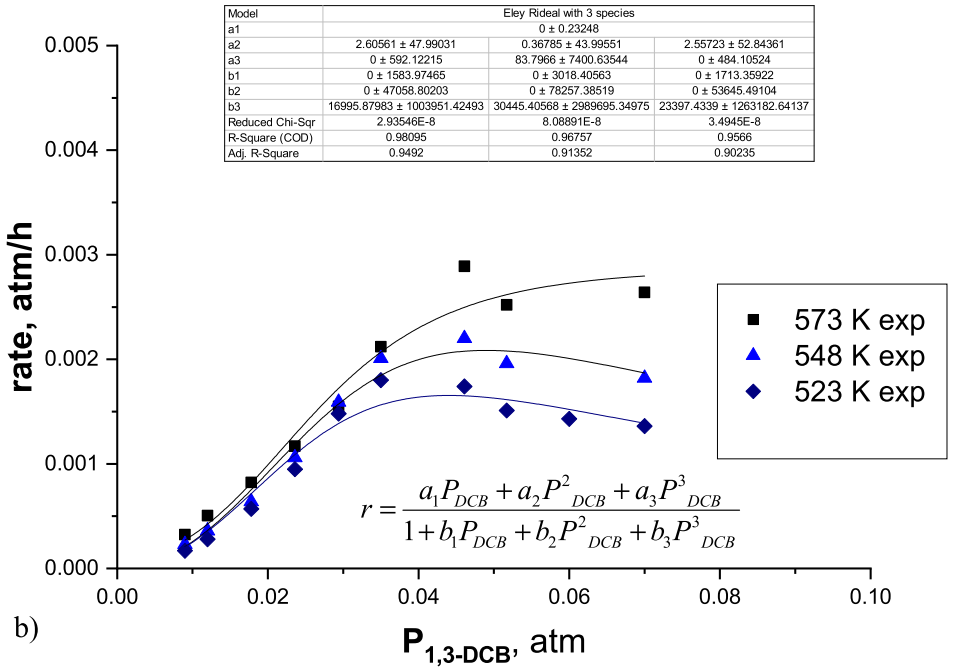

Fig. 6. Variation of experimental and calculated data for 1,3-dichlorobenzene hydrodechlorination rate as a function of reactant pressure at different temperatures for a case of 3 adsorbed species per cluster: a) Langmuir-Hinshelwood mechanism (Eq. (54)); b) Eley-Rideal mechanism.

$$S_{P_1} = \frac{r_{p_1}}{r_{p_1} + r_{p_2}} = \frac{k_A^{(1)} + 2k_{AA}^{(1)} C_A}{k_A^{(1)} + 2k_{AA}^{(1)} C_A + k_{AA}^{(2)} + 2k_{AA}^{(2)} C_A} = \frac{1}{1 + \frac{k_A^{(2)}}{k_A^{(1)}} \frac{(1 + \frac{2k_{AA}^{(2)} C_A^0}{k_A^{(2)}}(1-\delta))}{(1 + \frac{2k_{AA}^{(1)} C_A^0}{k_A^{(1)}}(1-\delta))}} = \frac{1}{1 + p_1 \frac{(1 + p_2(1-\delta))}{(1 + p_3(1-\delta))}} \quad (63)$$

where C_A^0 is the initial concentration of substrate A, $p_1 = k_A^{(2)}/k_A^{(1)}$; $p_2 = 2k_{AA}^{(2)} C_A^0 / k_A^{(2)}$; $p_3 = 2k_{AA}^{(1)} C_A^0 / k_A^{(1)}$ and δ is conversion.

It follows from Eq. (63) that selectivity approaches a limiting value $1/(1 + k_A^{(1)}/k_A^{(2)})$ at high conversion (a low substrate concentration) and depends on the initial substrate concentration at low conversion according to the following expression $S_{P_1} = 1/(1 + \left[(k_A^{(2)} + 2k_{AA}^{(2)} C_A^0)/(k_A^{(1)} + 2k_{AA}^{(1)} C_A^0)\right]$. This behavior is clearly different from the conventional case of parallel reaction when selectivity is independent on conversion for reactions of the same order being also independent on the initial substrate concentration (Murzin and Salmi, 2016).

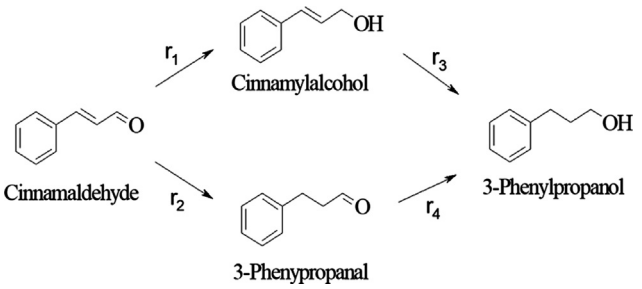

Fig. 7. Reaction network for cinnamaldehyde hydrogenation.

As an example of selectivity changes in parallel reactions with conversion increase hydrogenation of cinnamaldehyde (Fig. 7) on different ruthenium catalysts can be mentioned (Hajek et al., 2003; Hajek et al., 2003), where selectivity changes in parallel hydrogenation reactions were explained by in-situ formation of selective sites (Hajek et al., 2003). While such explanation can be valid for supported on silica ruthenium catalysts promoted with tin, creation of such sites for reduced un-promoted Ru on SiO_2, MCM-41 or zeolite Y is difficult to rationalize.

Fig. 8 illustrates applicability of the treatment above (Eq. (63)) to fit the selectivity data for hydrogenation of cinnamaldehyde on reduced ruthenium catalysts supported on a range of oxides.

In this reaction the starting compound with two functional groups (i.e. C = O and C = C) is hydrogenation in a parallel fashion to respectively cinnamyl alcohol and 3-phenylpropanal. Further hydrogenation of these intermediates to 3-phenylpropanol occurs at rather high conversion levels and can be neglected for the sake of clarity.

As can be seen in Fig. 8 Eq. (63) is able to explain a minor selectivity increase with conversion for Ru/MCM-41 with a relatively large particle size of ca. 20 nm even if some systematic deviations are visible.

The same approach clearly fails to adequately describe experimental data for other catalysts, showing a rather sharp increase of selectivity for especially Ru/Y-zeolite with the metal particle size in the range of 3.1–3.3 nm. Considering the dimensions of cinnamaldehyde (1.1 nm × 0.3 nm (Hajek et al., 2004) it is expected that several molecules of the substrate are able to adsorb on the surface of a single cluster. In a general case of several species adsorbed on a cluster and neglecting adsorption of products selectivity dependence can be obtained using Eq. (1):

$$S_{P_1} = \frac{r_{p_1}}{r_{p_1} + r_{p_2}} = \frac{a_1^{A->P_1} C_A + a_2^{A->P_1} C_A^2 + \ldots + a_n^{A->P_1} C_A^n}{a_1^{A->P_1} C_A + a_2^{A->P_1} C_A^2 + \ldots + a_n^{A->P_1} C_A^n + a_1^{A->P_1} C_A + a_2^{A->P_2} C_A^2 + \ldots + a_n^{A->P_2} C_A^n} \quad (64)$$

To avoid overparametrization Eq. (64) can be simplified considering only the terms with just one and the maximum number of adsorbed molecule on a cluster.

$$S_{P_1} = \frac{1}{1 + \frac{a_1^{A->P_2} C_A + a_n^{A->P_2} C_A^n}{a_1^{A->P_1} C_A + a_n^{A->P_1} C_A^n}} = \frac{1}{1 + \frac{a_1^{A->P_2}}{a_1^{A->P_1}} \frac{(1 + \frac{a_n^{A->P_2} (C_A^0)^{n-1}}{a_1^{A->P_2}} (1-\delta)^{n-1})}{(1 + \frac{a_n^{A->P_1} (C_A^0)^{n-1}}{a_1^{A->P_1}} (1-\delta)^{n-1})}} = \frac{1}{1 + p_1 \frac{(1 + p_4(1-\delta)^{p_5})}{(1 + p_6(1-\delta)^{p_5})}} \quad (65)$$

With

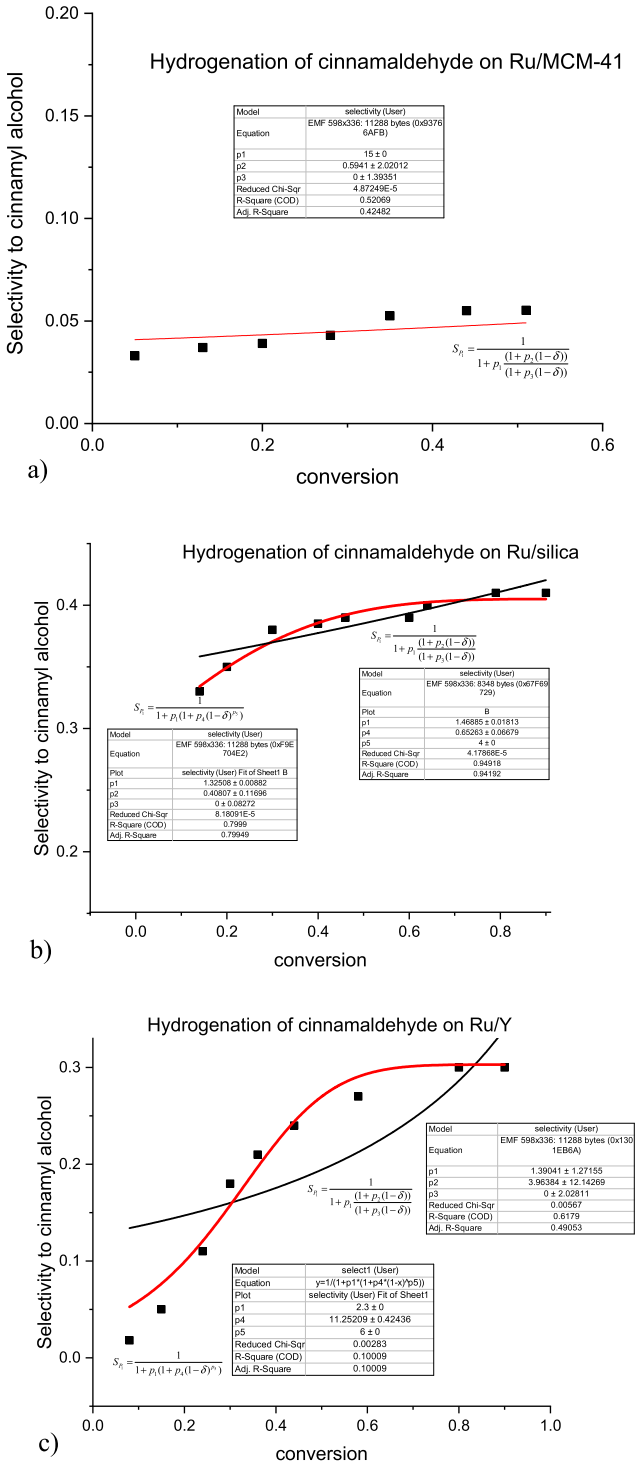

Fig. 8. Selectivity to cinnamylalcohol dependence on conversion for hydrogenation of cinnamaldehyde on ruthenium supported on a) MCM-41 (Hajek et al., 2003), b) silica (Hajek et al., 2003), c) Y zeolite (Hajek et al., 2003). Reactions were performed under total pressure of 5 MPa and 373 K for Ru/MCM-41 and Ru/Y-zeolite, and 7 MPa and 433 K for Ru/SiO_2.

$$p_4 = \frac{a_n^{A->P_2} (C_A^0)^{n-1}}{a_1^{A->P_2}}; \quad p_5 = n - 1; \quad p_6 = \frac{a_n^{A->P_1} (C_A^0)^{n-1}}{a_1^{A->P_1}} \quad (66)$$

Preliminary data fitting indicated that p_6 can be even neglected (Fig. 7c) resulting in the following three-parameter expression for selectivity to cinnamylalcohol:

$$S_{P_1} = \frac{1}{1 + p_1(1 + p_4(1-\delta)^{p_5})} \tag{67}$$

which was able to adequately describe the experimental data with physically and mathematically reasonable values of parameters. Namely at elevated conversion levels selectivity reached the value$S_{P_1} = 1/(1 + p_1)$, while according to the calculations up to 7 molecules of cinnamaldehyde are present simultaneously on a catalytically active ruthenium cluster of ca. 3 nm size.

6. Selectivity in consecutive reactions

The final example is related to consecutive reactions.

where the type of adsorbed species can be presented in a way similar to Fig. 3. The concentration of clusters with adsorption of either of the reactants is defined also by Eq. (48). Similar to the case of the parallel reactions the lateral interactions can be neglected for the sake of simplicity giving the following expressions for concentrations of different nanoclusters and the fraction of bare clusters:

$$\begin{aligned} f_{0A} &= K_A f_{00} C_A f_{AA} = (K_A C_A)^2 f_{00} f_{0B} = K_B C_B f_{00} f_{BB} \\ &= (K_B C_B)^2 f_{00} f_{AB} = K_A K_B f_{00} C_A C_B \end{aligned} \tag{68}$$

$$f_{00} = \frac{f_{total}}{1 + K_A C_A + (K_A C_A)^2 + K_B C_B + (K_B C_B)^2 + K_A K_B C_A C_B} \tag{69}$$

The reaction rate for the transformation of A to B can be written as:

$$r_{A->B} = k_{A->B}(f_A + f_{AA} + f_{AB})/f_{total} \tag{70}$$

considering that transformations of the cluster of AA type (Fig. 3) occur stepwise through a cluster AB and that the rate constant does not depend on the presence of other species adsorbed on that cluster. In a similar way the rate expression for the second route in the overall reaction network:

$$r_{B->C} = k_{B->C}(f_B + f_{AB} + f_{BB})/f_{total} \tag{71}$$

giving thus an expression for differential selectivity S_B^{diff} towards the reactant *B:*

$$\begin{aligned} S_B^{diff} &= \frac{dC_B}{-dC_A} = \frac{r_{A->B} - r_{B->C}}{r_{A->B}} = 1 - \frac{r_{A->B} - r_{B->C}}{r_{A->B}} = 1 - \frac{k_{B->C}(f_B + f_{AB} + f_{BB})}{k_{A->B}(f_A + f_{AA} + f_{AB})} \\ &= 1 - \frac{k_{B->C} K_B C_B}{k_{A->B} K_A C_A} \frac{1 + K_B C_B + K_A C_A}{1 + K_A C_A + K_B C_B} = 1 - \frac{k_{B->C} K_B C_B}{k_{A->B} K_A C_A} \end{aligned} \tag{72}$$

which is the same as in the conventional treatment of consecutive reactions (Murzin and Salmi, 2016). On the contrary, when the rate and adsorption constants depend on the presence of other species on the surface, instead of Eq. (72) one gets for differential selectivity:

$$\begin{aligned} S_B^{diff} &= \frac{dC_B}{-dC_A} = 1 - \frac{k^{0B}_{B->C} f_{0B} + k^{AB}_{B->C} f_{AB} + k^{BB}_{B->C} f_{BB}}{k^{0A}_{A->B} f_{0A} + k^{AA}_{A->B} f_{AA} + k^{AB}_{A->B} f_{AB}} = \\ &= 1 - \frac{k^{0B}_{B->C} K_{0B} C_B}{k^{0A}_{A->B} K_{0A} C_A} \frac{1 + \frac{k^{AB}_{B->C}}{k^{0B}_{B->C}} K_{AB} K_{BA} C_A + \frac{k^{BB}_{B->C}}{k^{0B}_{B->C}} K_{BB} C_B}{1 + \frac{k^{AA}_{A->B}}{k^{0A}_{A->B}} K_{AA} C_A + \frac{k^{AB}_{A->B}}{k^{0A}_{A->B}} \frac{K_{AB} K_{BA}}{K_{0A}} C_B} \end{aligned} \tag{73}$$

which in a general case cannot be reduced to the final expression in Eq. (72).

An analytical solution of Eq. (73) is very tedious, thus numerical data fitting can be considered as the primary option to elucidate the differences in selectivity behavior for nanoconfined cases compared to a conventional Langmuir approach.

Tractable analytical solutions, however, can be obtained for some physically reasonable cases considering for example strong adsorption of the reactant *A*. If the concentration of the clusters with mixed adsorbates (i.e. *AB* type) dominates over other clusters with the reactant B, leading to $k^{AB}_{B->C} f_{AB} >> k^{BB}_{B->C} f_{BB} + k^{0B}_{B->C} f_{0B}$ and at the same time the following relationship is valid$(k^{0A}_{A->B} f_{0A} + k^{AA}_{A->B} f_{AA}) >> k^{AB}_{A->B} f_{AB}$, Eq. (73) gives:

$$\begin{aligned} -\frac{dC_B}{dC_A} &= 1 - \frac{k^{AB}_{B->C} f_{AB}}{k^{0A}_{A->B} f_{0A} + k^{AA}_{A->B} f_{AA}} \\ &= 1 - \frac{k^{AB}_{B->C} K_{AB} K_{BA} C_B}{k^{0A}_{A->B} K_{0A} (1 + \frac{k^{AA}_{A->B}}{k^{0A}_{A->B}} K_{AA} C_A)} \end{aligned} \tag{74}$$

Which can be transformed to:

$$\frac{dC_B}{dC_A} + C_B\left(-\frac{k^{AB}_{B->C} K_{AB} K_{BA}}{k^{0A}_{A->B} K_{0A} (1 + \frac{k^{AA}_{A->B}}{k^{0A}_{A->B}} K_{AA} C_A)}\right) = -1 \tag{75}$$

Or an equation of the type:

$$y' + yP(x) = Q \tag{76}$$

with$y = C_B, x = C_A$, $Q = -1$ and $P(x) = -b/[1 + ax]$ where:

$$a = \frac{k^{AA}_{A->B}}{k^{0A}_{A->B}} K_{AA}; b = \frac{k^{AB}_{B->C} K_{AB} K_{BA}}{k^{0A}_{A->B} K_{0A}} \tag{77}$$

The solution for the differential equation $y' + yP(x) = Q$ is:

$$y = e^{-\int P dx}\left[\int Q e^{\int P dx} dx + C'\right] \tag{78}$$

which after some manipulations gives:

$$y = \frac{1}{a-b}\left[\frac{(1+ax)^{b/a}}{(1+ax_0)^{b/a-1}} - (1+ax)\right] \tag{79}$$

or

$$C_B = \frac{1}{a-b}\left[\frac{(1+aC_A)^{b/a}}{(1+aC_A^0)^{b/a-1}} - (1+aC_A)\right] \tag{80}$$

where C_A^0 corresponds to the initial concentration of reactant A. For the classical treatment of Langmuirian (ideal) surfaces when$1 << aC_A$, Eq. (80) is reduced to the well-known expression for the concentration of the intermediate component in a consecutive reaction network reported previously (Murzin and Salmi, 2016), namely:

$$C_B = \frac{1}{1 - \frac{b}{a}}\left[\frac{(C_A)^{b/a}}{(C_A^0)^{b/a-1}} - C_A)\right] \tag{81}$$

The integral selectivity towards the intermediate component S_B^{int} in the conventional case of the Langmuir approach is as follows,

$$S_B^{int} = \frac{C_B}{C_A^0 - C_A} = \frac{1}{(a-b)(C_A^0 - C_A)}\left[\frac{(aC_A)^{b/a}}{(aC_A^0)^{b/a-1}} - aC_A\right] \tag{82}$$

which can be expressed as a function of conversion δ:

$$\begin{aligned} S_B^{int} &= \frac{\frac{1}{aC_A^0}}{(1 - \frac{b}{a})\delta}\left[\frac{(aC_A^0(1-\delta))^{b/a}}{(aC_A^0)^{b/a-1}} - aC_A^0(1-\delta)\right] \\ &= \frac{1}{(1 - \frac{b}{a})}\left[\frac{(1-\delta)^{b/a} - (1-\delta)}{\delta}\right] \end{aligned} \tag{83}$$

Or in the form reported previously in (Murzin and Salmi, 2016):

$$S_B^{int} = \frac{1}{1-b/a}\frac{1}{\delta}\left[(1-\delta)^{b/a} - (1-\delta)\right] \quad (84)$$

With $b/a = k_{B->C}K_B/k_{A->B}K_A$.

For selectivity towards the intermediate compounds corresponding to a case with two adsorbed molecules per cluster or in a nanoconfined space, it can be written considering Eq. (81) that

$$S_B^{int} = \frac{C_B}{C_A^0 - C_A} = \frac{1}{(a-b)(C_A^0 - C_A)}\left[\frac{(1+aC_A)^{b/a}}{(1+aC_A^0)^{b/a-1}} - (1+aC_A)\right] \quad (85)$$

which can be transformed into

$$S_B^{int} = \frac{1}{(1-\frac{b}{a})}\left[\frac{(1+aC_A^0(1-\delta))^{b/a}}{\delta aC_A^0(1+aC_A^0)^{b/a-1}} - \frac{(1+aC_A^0(1-\delta))}{\delta aC_A^0}\right] \quad (86)$$

and further

$$S_B^{int} = \frac{1}{(1-b/a)\delta}\left[\frac{(1+aC_A^0(1-\delta))^{b/a}}{aC_A^0(1+aC_A^0)^{b/a-1}} - \frac{1}{aC_A^0} - (1-\delta)\right] \quad (87)$$

Eq. (87) by setting $1 << aC_A$ is reduced to Eq. (84) describing integral selectivity dependence of the intermediate as a function of conversion for the classical treatment.

An interesting observation, stemming from Eq. (87), is the dependence of selectivity not only on conversion and the b/a ratio, which is trivial, but also on the initial concentration of the reactant A. A similar behavior was noticed in a recent numerical treatment of selectivity for networks comprising consecutive reactions of the second and the first order (Murzin et al., 2019). Reductive amination of aldehydes comprising formation of the imine and subsequent hydrogenation under hydrogen excess or the Prins condensation reaction followed by dehydration of the primary condensation were considered as chemically relevant examples of processes, where a bimolecular reaction is followed by a monomolecular one. The experimental data on the preparation of octahydro-2H-chromen-4-ol with analgesic activity from isopulegol and thiophene-2-carbaldehyde in the presence of acid-modified clays clearly showed that selectivity to the intermediate product was dependent on the initial reactant concentration. The latter was regulated by the solvent addition (Sidorenko et al., 2018).

In (Murzin et al., 2019) numerical simulations were conducted, illustrating that selectivity towards the intermediate compound strongly depends on the initial concentration of the substrate. It should be noted that because of the linearity of the system of differential equations for the first order reactions, mainly they are considered in textbooks on chemical kinetics providing analytical solutions for concentration profiles (Laidler, 1987; Arnaut et al., 2006) and subsequently selectivity, while an analytical treatment of more complex cases is far from being trivial.

In fact, the exact solution for a mixed second order network contains hypergeometric functions (Kiss and Osz, 2017; Lente, 2015) being too complicated for a meaningful analysis of selectivity dependence on conversion.

The considerations above presented for a special case, when Eq. (72) could be simplified, allowed an analytic solution (i.e. Eq. (87)) explicitly illustrating that selectivity to the intermediate compound depends on the initial concentration. Visualization of such dependence is given in Fig. 9.

At a low value of the b/a ratio selectivity to the intermediate B is very high, nevertheless an increase in the initial substrate concentration result in a decrease of selectivity at the same conversion level (i.e. b/a = 0.2, aC^0 = 0.5 vs b/a = 0.2, aC^0 = 5). A further increase of the initial concentration (i.e. b/a = 0.2, aC^0 = 5 vs b/a = 0.2, aC^0 = 10) does not significantly influence the selectivity profile. A similar behavior is observed for another set of parameters with b/a = 2, where a low initial substrate concentration leads to high activity, while concentrated solutions give a drastic decline in selectivity somewhat levelling off upon a further increase of the initial substrate concentration.

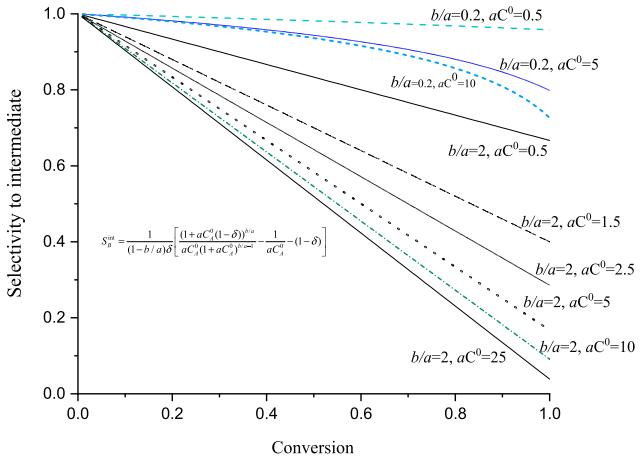

Fig. 9. Dependence of selectivity to the intermediate product as a function of conversion for different values of parameters for Eq. (87).

It is interesting to compare at least conceptually the theoretical considerations above with available experimental data. Data for a parallel consecutive network (Fig. 10a), namely hydrogenation of crotonaldehyde over $IrRe/Al_2O_3$ catalyst), clearly illustrate that selectivity to the intermediate product crotyl alcohol decreases with an increase of the initial substrate concentration (Fig. 10b). Somewhat similar behavior was reported for the same reaction over Pt/K10 catalyst (Kun et al., 2001), where an increase of the initial crotonaldehyde concentration resulted in a decrease of selectivity to crotyl alcohol for the experimental data obtained at the same conversion level (Kun et al., 2001). Apparently, a detailed regression analysis is required for a quantitative comparison of the theoretical approach developed in the current work with the available experimental data on crotonladehyde hydrogenation and similar reactions.

Note that, as can be concluded from Fig. 10c, formation of butanol starts almost from the beginning of the reaction, thus the combined selectivity to semi-hydrogenation products (i.e. crotyl alcohol and butanal) is mediocre. Subsequently, an assumption on the presence of metal clusters bearing not only the substrate, but also the semi-hydrogenated product, is chemically reasonable.

A different situation can be anticipated for hydrogenation of alkyne where selectivity over palladium catalysts is typically very high. Experimental data on the triple bond hydrogenation in various alkynes (e.g. phenyl- and diphenylacetylene, 1-phenyl-1-propyne) over single-atom alloy palladium catalysts as well as over supported Pd nanoparticles were reported in (Markov et al., 2019; Markov et al., 2021; Rassolov et al., 2021; Rassolov et al., 2021). Profiles of selectivity to olefins as a function of conversion on a single-atom alloy catalyst did not change when the initial substrate concentration was altered, which can be anticipated, as there is no space for a second substrate molecule to adsorb on the single-atom active site. On the contrary, for supported palladium nanoparticles it was observed (Rassolov et al., 2021) that higher initial concentrations of the alkyne resulted in higher selectivity to the corresponding olefin at the same conversion level.

Similar results were obtained in (Wu et al., 2017) for hydrogenation of phenylacetylene. Apparently, not all assumptions aimed at simplification of Eq. (73) in the case of triple bond hydro-

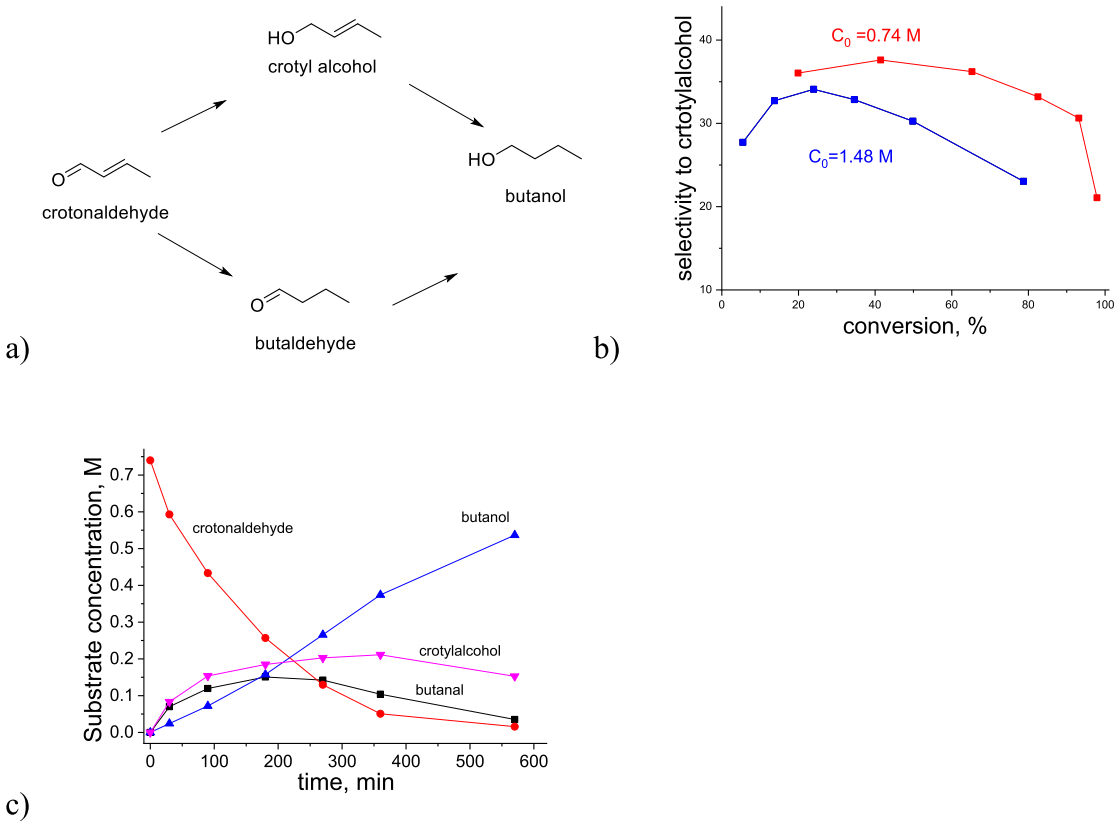

Fig. 10. Hydrogenation of crotonaldehyde at 1.15 MPa and 453 K over $IrRe/Al_2O_3$ catalyst: a) reaction network, b) selectivity to crotyl alcohol c) concentration profiles (Simakova).

genation are thus valid. An alternative explanation still assuming that the terms containing the concentration of the olefin (i.e. $(k^{BB}_{B->C}/k^{0B}_{B->C})K_{BB}C_B$ and $(k^{AB}_{A->B}/k^{0A}_{A->B})(K_{AB}K_{BA}/K_{0A})C_B)$ can be neglected, implies that presence of the alkyne strongly hinders adsorption of the intermediate olefin. Such suggestion is in line with a recent study on the adsorption of 2-methyl-3-butyn-2-ol, an alkyne alcohol and its corresponding semi-hydrogenated alkyne alcohol (Cherkassov et al., 2021). Adsorption experiments combined with theoretical studies revealed existence of alkyne sites on Pd catalysts, which strongly adsorb the alkyne and only weakly the corresponding alkene. Subsequently Eq. (73) can be transformed to:

$$S_B^{diff} = 1 - M\frac{C_B}{C_A(1+aC_A)} \tag{88}$$

With

$$M = \frac{k^{0B}_{B->C}K_{0B}}{k^{0A}_{A->B}K_{0A}}a = \frac{k^{AA}_{A->B}}{k^{0A}_{A->B}}K_{AA} \tag{89}$$

The analytical solution of Eq. (88) is rather cumbersome:

$$C_B = Ge^{M(\ln C_A - \ln(aC_A+1))} + \frac{C_A(aC_A+1)_2^{-M}F_1(1-M,-M;2-M;-aC_A)}{M-1} \tag{90}$$

where G is determined from the boundary conditions (e.g. $C_B = 0$ when $C_A = C_A^0$) and ${}_2F_1(1-M,-M;2-M;-aC_A)$ is the hypergeometric function.

Even a simplified version of Eq. (88) assuming1 << aC_A:

$$S_B^{diff} = 1 - M'\frac{C_B}{C_A^2} \tag{91}$$

With

$$M' = M/a = \frac{k^{0B}_{B->C}K_{0B}}{k^{AA}_{A->B}K_{0A}K_{AA}} \tag{92}$$

gives a complicated analytical solution

$$C_B = Ge^{-M'/C_A} + (M')e^{-M'/C_A}Ei(M'/C_A) - C_A \tag{93}$$

Apparently, Eqs. (90) or (93) cannot be used in a straightforward way for elucidation of the selectivity behavior depending on the kinetic parameters and the initial substrate concentration.

For an adequate description of the experimental data for diphenylacetylene hydrogenation over a supported Pd nanocatalyst displaying selectivity dependence on the initial reactant concentration at the same conversion level, it was suggested in (Rassolov et al., 2021) that from at least the mathematical viewpoint the denominators in the rate equations for hydrogenation of the alkyne and alkenes cannot be the same. Namely, it was assumed (Rassolov et al., 2021), that hydrogenation of an alkyne follows the Eley-Rideal mechanism, while the Langmuir-Hinshelwood mechanism is operative for olefins hydrogenation giving the following equations using notation of the current study without considerations of the hydrogen pressure dependences:

$$r_{A->B} = \frac{k_1K_AC_A}{1+K_AC_A+K_BC_B}r_{B->C} = \frac{k_2K_BC_B}{(1+K_AC_A+K_BC_B)^2} \tag{94}$$

For this case the differential selectivity is

$$S_B^{diff} = \frac{dC_B}{-dC_A} = 1 - \frac{k_2K_BC_B}{k_1K_AC_A(1+K_AC_A+K_BC_B)} \tag{95}$$

which is remarkably similar to Eq. (88) when neglecting the term K_BC_B because of the weak olefin adsorption. As mentioned above,

eqns. of the type (94) were successfully applied in (Rassolov et al., 2021) to account for selectivity behavior in diphenylacetylene hydrogenation.

An alternative explanation proposed in the current study arrives at the same mathematical form of the selectivity dependence on the initial substrate concentration, suggesting presence of metal nanoclusters on the catalyst surface with at least two adsorbed alkyne molecules on a single cluster.

To illustrate selectivity dependence on the initial concentration numerical analysis of Eq. (91) was performed by transforming it first into the differential equation:

$$\frac{dC_B}{d\delta} = C_A^0 - \frac{M' C_B}{(1-\delta)^2 C_A^0} \tag{96}$$

where δ is conversion, and then solving it numerically in Matlab for different values of M' and C_A^0. As can be seen from Fig. 11, higher ini-

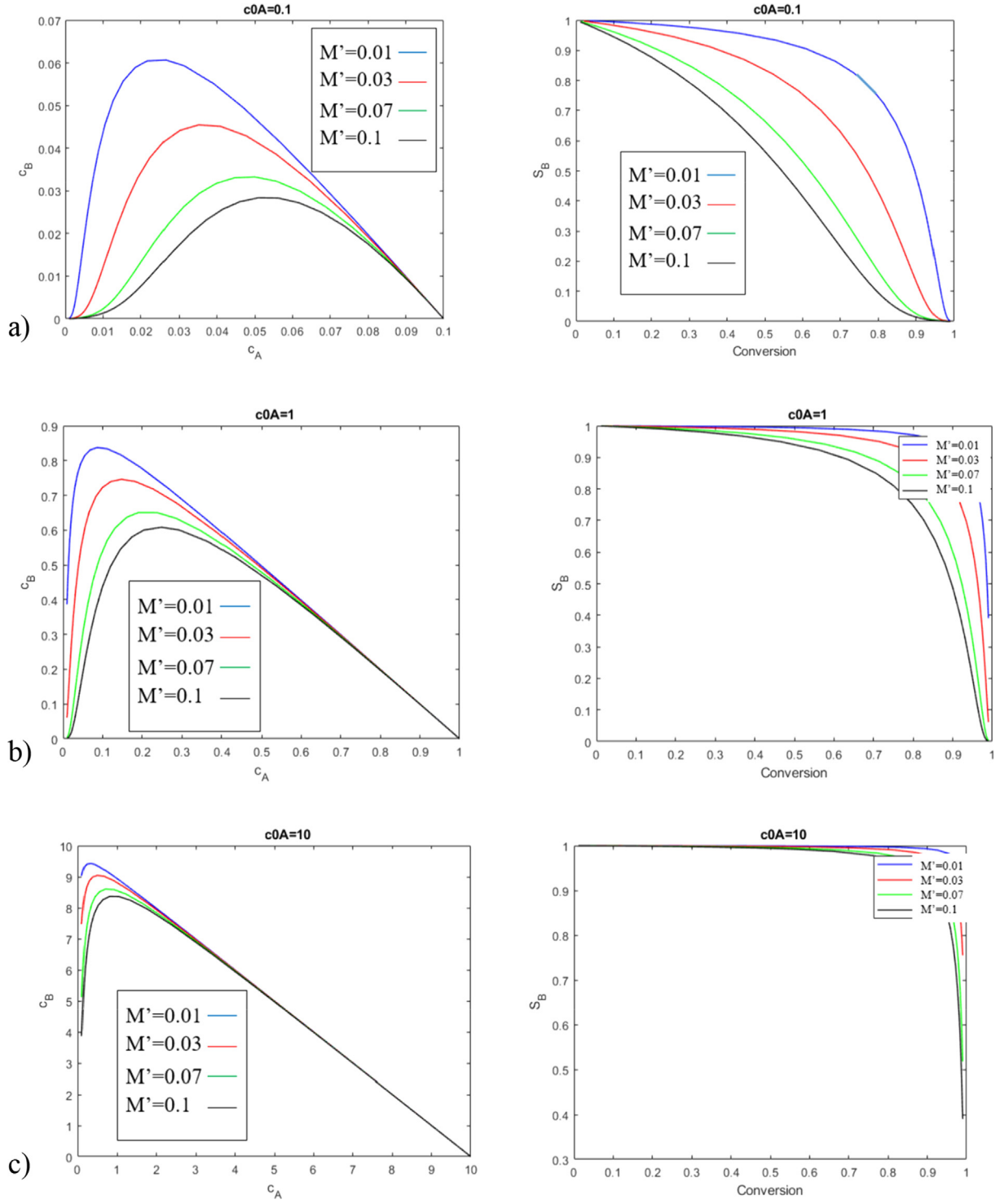

Fig. 11. Dependence of the intermediate product concentration on the substrate concentration (left) and selectivity to the intermediate product as a function of conversion (right) for different values of the initial substrate concentration C_A^0 (a.u.) a) 0.1; b) 1, c) 10.

tial substrate concentrations lead to higher selectivity towards the intermediate olefin having a good conceptual agreement with the experimental data on selective hydrogenation of alkynes.

7. Conclusions

An approach to kinetics on nanoclusters, when dimensions of adsorbed molecules are comparable in size with the nanoclusters, developed previously for the monomolecular reactions on catalytic surfaces, was extended to Eley-Rideal, Langmuir-Hinshelwood and two-step sequence reaction mechanisms, by assuming adsorption of several molecules of different type on a single metal cluster/catalytic ensemble. Lateral interactions were considered via dependence of adsorption parameters on the composition of the adsorbed layer, distinguishing clusters with both reactants adsorbed through different sequences of adsorption steps.

For the Eley-Rideal mechanism depending on the values of the rate and adsorption constants, the forward rate can follow a second order in the starting reactant. Even a maximum in the rate upon an increase in the same reactant concentration is possible. In the case of the two-step sequence implying existence of just one most abundant surface intermediate, the overall order to both reactants for the reactions in a nanoconfined space is equal to unity similar to the classical Langmuir approach. Kinetic behavior for the Langmuir-Hinshelwood mechanism becomes different from the mean field approximation when at least three species can be adsorbed per cluster. Applicability of this mechanism is illustrated for catalytic hydrodechlorination of 1.3-dichlorobenzene on nickel clusters of ca. 1.4 nm size.

For parallel reactions of the Eley-Rideal type selectivity depends on conversion for the overall chemical reactions of the same order as a result of the cooperative behaviour of two adsorbed molecules of a reactant per cluster. Comparison between the theory and experiments was done for hydrogenation of cinnamaldehyde on supported ruthenium clusters. A sharp increase of selectivity vs conversion observed experimentally for ruthenium supported on zeolite Y implies that up to seven molecules of the reactant can be adsorbed per cluster of ca. 3 nm size.

Cooperative behavior for consecutive reactions results in the selectivity to the intermediate product dependence on the initial substrate concentration in contrast to the mean field approximation. Case studies where such kinetic behavior was observed include hydrogenation of crotonaldehyde and alkynes.

CRediT authorship contribution statement

Dmitry Yu. Murzin: Conceptualization, Investigation, Writing – original draft.

Declaration of Competing Interest

The authors declare that they have no known competing financial interests or personal relationships that could have appeared to influence the work reported in this paper.

Acknowledgements

The author is grateful to Prof. J. Wärnå for numerical analysis of Eq. (91) using Matlab. Dr. I. Simakova is acknowledged for sharing experimental data on crotonaldehyde hydrogenation.

References

Arnaut, L., Formosinho, S., Burrows, H., 2006. Chemical Kinetics. Elsevier, Amsterdam.
Astruc, D., 2020. Chem. Rev. 120, 461.
Augustine, R.L., 2016. Catal. Let. 146, 2393.
Bär, M., Gottschalk, N., Eiswirth, M., Ertl, G., 1994. J. Chem. Phys. 100, 1202–1212.
Bell, A.T., 2003. Science 299, 688.
Boreskov, G.K., Fiz. Khim., Z.h., 1945. J. Phys. Chem. (USSR) 19, 92. in Russian.
Boudart, M., Tamaru, K., 1991. Catal. Lett. 9, 15.
Burda, C., Chen, X., Narayanan, R., El-Sayed, M.A., 2005. Chem. Rev. 105, 1025.
Chen, P., Zhou, X., Andoy, N.M., Han, K.-S., Choudhary, E., Zou, N., Chen, G., Shen, H., 2014. Chem. Soc. Rev. 43, 1107.
Cherkassov, N., Murzin, D.Y., Catlow, C.R.A., Chutia, A., 2021. Catal. Sci. Tech. 11, 6205.
Cui, Q., Karplus, M., 2008. Protein Sci. 17, 1295.
Dong, B., Pei, Y., Mansour, N., Lu, X., Yang, K., Huang, W., Fang, N., 2019. Nat. Commun. 10, 4815.
Dong, B., Mansour, N., Pei, Y., Wang, Z., Huang, T., Filbrun, S.L., Chen, M., Cheng, X., Pruski, M., Huang, W., Fang, N., 2020. J. Am. Chem. Soc. 142, 13305.
Fogler, H.S., 1998. Elements of Chemical Reaction Engineering. Prentice Hall, NJ.
Fokin, S.J., 1913. J. Russ. Phys. Chem. Soc 45, 286.
Hajek, J., Kumar, N., Mäki-Arvela, P., Salmi, T., Murzin, D.Y., Paseka, I., Heikkilä, T., Laine, E., Laukkanen, P., Väyrynen, J., 2003. Appl. Catal. A. 251, 385.
Hajek, J., Kumar, N., Salmi, T., Murzin, D.Y., Karhu, H., Väyrynen, J., Cerveny, L., Paseka, I., 2003. Ind. Eng. Chem. Res. 42, 295.
Hajek, J., Kumar, N., Nieminen, V., Mäki-Arvela, P., Salmi, T., Murzin, D.Y., Cerveny, L., 2004. Chem. Eng. J. 103, 35–43.
Helfferich, F.G., 2001. Kinetics of Homogeneous Multistep Reactions. In: Compton, R.G., Hancock, G. (Eds.), Comprehensive chemical kinetics, vol. 38. Elsevier, Amsterdam.
Henry, C.R., 2000. Appl. Surf. Sci. 164, 252.
Horiuti, J., Enomoto, S., 1953. Proc. Japan Acad. 29, 164.
Kaiser, S.K., Chen, Z., Faust Akl, D., Mitchell, S., Pérez-Ramírez, J., 2020. Chem. Rev. 120, 11703.
Kapteijn, F., Berger, R.J., Moulijn, J.A., 2008. Rate procurement and kinetic modelling. Handbook of Heterogeneous Catalysis. https://doi.org/10.1002/9783527610044.hetcat0092, Wiley.
Keane, M.A., Murzin, D.Y., 2001. Chem. Eng. Sci. 56, 3185.
Keane, M.A., Murzin, D.Y., 2002. Catal. Org. React. 89, 595.
Kiss, V., Osz, K., 2017. Int. J. Chem. Kinet. 49, 602.
Kou, S.C., Cherayil, B.J., Min, W., English, B.P., Xie, X.S., 2005. J. Phys. Chem. B 109 (41), 19068.
Kun, I., Szöllösi, G., Bartok, M., 2001. J. Mol. Cat. A: Chem. 169, 235.
Laidler, K.J., 1987. Chemical Kinetics. Pearson Education, NY.
Lazman, M.Z., Yablonsky, G.S., 2008. Adv. Chem. Eng. 34, 47.
Lente, G., 2015. J. Math. Chem. 53, 1172.
Leskovac, V., 2003. Comprehensive Enzyme Kinetics. Kluwer Academic/Plenum Publishers, New York.
Levenspiel, O., 1999. Chemical Reaction Engineering. John Wiley & Sons, New York.
Ligthart, D.A.J.M., van Santen, R.A., Hensen, E.J.M., 2011. J. Catal. 280, 206.
Liu, L., Corma, A., 2021. Chem 7, 1.
Lu, H.P., Xun, L., Xie, X.S., 1877. Science 1998, 282.
Marin, G., Yablonsky, G.S., Constales, D., 2019. Kinetics of Chemical Reactions, Decoding complexity. Wiley.
Markov, P.V., Mashkovsky, I.S., Bragina, G.O., Wärnå, J., Gerasimov, E.V., Bukhtiyatov, V.I., Stakheev, A.Y., Murzin, D.Y., 2019. Chem. Eng. J. 358, 520–530.
Markov, P.V., Mashkovsky, I.S., Bragina, G.O., Wärnå, J., Bukhtiyarov, V.I., Stakheev, A.Yu., Murzin, D.Yu., 2021. Chem. Eng. J. 404. 126409 (1-11).
Murzin, D.Y., 2007. React. Kinet. Catal. Lett. 91, 37.
Murzin, D.Y., 2010. J. Catal. 276, 85–91.
Murzin, D.Y., 2010. Langmuir 26, 4854.
Murzin, D.Y., 2020. Engineering Catalysis. DeGruyter, Berlin.
Murzin, D.Y., Salmi, T., 2016. Catalytic Kinetics, Chemistry and Engineering. Elsevier.
Murzin, D.Y., Simakova, I.L., Wärnå, J., 2019. Int. J. Chem. Reactor Eng. 17, 20180161.
Narayanan, R., El-Sayed, M.A., 2008. Top. Catal. 47, 15.
Punia, B., Chaudhury, S., Kolomeisky, A.B., 2022. PNAS 119, (3) e2115135119.
Rassolov, A.V., Mashkovsky, I.S., Bragina, G.O., Baeva, G.N., Markov, P.V., Smirnova, N.S., Wärnå, J., Stakheev, A.Y., Yu Murzin, D., 2021. Mol. Catal. 506, 111550.
Rassolov, A.V., Mashkovsky, I.S., Baeva, G.N., Bragina, G.O., Smirnova, N.S., Markov, P.V., Wärnå, J., Bukhtiyarov, A.V., Stakheev, A.Y., Murzin, D.Y., 2021. Nanomater. 11, 3286.
Razdan, N.K., Bhan, A., 2021. PNAS 118, e2019055118.
Razdan, N.K., Bhan, A., 2021. J. Catal. 404, 726–744.
Rotermund, H.H., Engel, W., Kordesch, M., Ertl, G., 1990. Nature 343, 355–356.
Sabatier, P., 2022. Catalysis in Organic Chemistry. Van Nostrand, New York.
Salmi, T.O., Mikkola, J.-P., Wärnå, J., 2010. Chemical Reaction Engineering and Reactor Technology. CRC Press.
Samantaray, M.K., D'Elia, V., Pump, E., Falivene, L., Harb, M., Chikh, S.O., Cavallo, L., Basset, J.M., 2020. Chem. Rev. 120 (2), 734.
Santen, R.A., 2009. Acc. Chem. Res. 42, 57.
Schlögl, R., Abd Hamid, S.B., 2004. Angew. Chem. Int. Ed. 43, 1628.
Sidorenko, A.Y., Kravtsova, A.V., Wärnå, J., Aho, A., Heinmaa, I., Il'ina, V., Volcho, K.P., Salakhutdinov, N.F., Murzin, D.Yu., Agabekov, V.E., 2018. Mol. Catal. 453, 139.
Siffert, S., Murzin, D.Y., Garin, F., 1999. Appl. Catal. A. Gen. 178, 85.
Simakova, I.L. Personal communication to the author.
Somorjai, G.A., Frei, H., Park, J.Y., 2009. J. Am. Chem. Soc. 131, 16589.
Temkin, M.I., 1963. Dokl. Akad. Nauk USSR 152, 156.
Temkin, M.I., 1979. Adv. Catal. 28, 173–291.

Temkin, M.I., 1984. *Kinet. Katal.* 25, 299.
Temkin, O.N., 2012. Homogeneous Catalysis with Metal Complexes: Kinetic Aspects and Mechanisms. Wiley, Weinheim.
Wu, Z., Calcio Gaudino, E., Manzoli, M., Martina, K., Drobot, M., Krtschil, U., Cravotto, G., 2017. Catal. Sci. Tech. 7, 4780.
Xu, W., Kong, J.S., Yeh, Y.T., Chen, P., 2008. Nat. Mater. 7, 992.
Yablonsky, G.S., Lazman, M.Z., 1997. Stud. Surf. Sci. Catal. 109, 371.
Ye, R., Mao, X., Sun, X., Chen, P., 1985. ACS Catal. 2019, 9.
Zhang, W., Fu, Q., Luo, Q., Sheng, L., Yang, J., 2021. JACS Au 1, 2130.
Zou, N., Zhou, X., Chen, G., Andoy, N.M., Jung, W., Liu, G., Chen, P., 2018. Nat. Chem. 10, 607.